**Bin Xie**
School of Energy and Power Engineering,
Huazhong University of Science and Technology,
Wuhan 430074, China

**Haochen Liu**
Department of Electrical and Electronic Engineering,
Southern University of Science and Technology,
Shenzhen 518055, China

**Xiao Wei Sun**
Department of Electrical and Electronic Engineering,
Southern University of Science and Technology,
Shenzhen 518055, China

**Xingjian Yu**
School of Energy and Power Engineering,
Huazhong University of Science and Technology,
Wuhan 430074, China

**Ruikang Wu**
School of Energy and Power Engineering,
Huazhong University of Science and Technology,
Wuhan 430074, China

**Kai Wang**
Department of Electrical and Electronic Engineering,
Southern University of Science and Technology,
Shenzhen 518055, China

**Xiaobing Luo**[1]
School of Energy and Power Engineering,
Huazhong University of Science and Technology,
Wuhan 430074, China
e-mail: luoxb@hust.edu.cn

# Reduced Working Temperature of Quantum Dots-Light-Emitting Diodes Optimized by Quantum Dots at Silica-on-Chip Structure

*White light-emitting diodes (WLEDs) composed of blue LED chip, yellow phosphor, and red quantum dots (QDs) are considered as a potential alternative for next-generation artificial light source with their high luminous efficiency (LE) and color-rendering index (CRI) while QDs' poor temperature stability and the incompatibility of QDs/silicone severely hinder the wide utilization of QDs-WLEDs. To relieve this, here we proposed a separated QDs@silica nanoparticles (QSNs)/phosphor structure, which composed of a QSNs-on-chip layer with a yellow phosphor layer above. A silica shell was coated onto the QDs surface to solve the compatibility problem between QDs and silicone. With CRI > 92 and R9 > 90, the newly proposed QSNs-based WLEDs present 16.7% higher LE and lower QDs working temperature over conventional mixed type WLEDs. The reduction of QDs' temperature can reach 11.5 °C, 21.3 °C, and 30.3 °C at driving current of 80 mA, 200 mA, and 300 mA, respectively.* [DOI: 10.1115/1.4042981]

*Keywords: light-emitting diodes, quantum dots, photo-thermal effect, geometric optical design*

## 1 Introduction

White light-emitting diodes (WLEDs) have been attracting numerous interests due to their extraordinary characteristics over conventional light sources such as high efficiency, low consumption, environmental protection, and long lifetime [1–3]. The most widely used phosphor-converted WLEDs (pc-WLEDs) are realized by combining blue LED chip with yellow-emissive $Y_3Al_5O_{12}:Ce^{3+}$ (YAG:Ce) phosphor. The pc-WLEDs can achieve high luminous efficiency (LE), while their color-rendering index (CRI) is relatively low (70) due to the lack of red spectral components [4]. Adding red phosphor is an effective way to remedy the defect of CRI. However, it is incapable of maintaining high LE because the broad red emission partially lies outside the sensitive region of human eyes [5,6].

Quantum dots (QDs), as down-conversion nanocrystals, have attracted attention due to their unique optical properties such as narrow emission spectrum, size-tunable emission wavelength, and high quantum yields [7]. It has been proved that adding QDs into pc-WLEDs can greatly improve CRI and color gamut, and QDs' narrow emission allows for the potential of high LE [8,9], making QDs-WLEDs a potential alternative for next-generation artificial light source [10]. However, there are two obstacles in the packaging of QDs-WLEDs. One is that the hydrophobic organic ligands on QDs' surface damage the polymerization of silicone gel, namely the catalyst poisoning effect [11]. Besides, the incompatibility of QDs' surface with silicone gel will result in QDs agglomeration, consequently decreasing the photoluminescence (PL) efficiency. Therefore, QDs cannot be directly mixed with phosphor–silicone gel. Another is the poor temperature stability of QDs, which makes QDs' photoluminescence decrease sharply with the increase of working temperature. Several solutions have been proposed to solve the compatibility problem, such as QDs' surface chemistry modification [12,13], incorporating QDs into mesoporous microspheres [14], and coating silica barrier layer on QDs' surface [15,16], Although the compatibility between QDs-silica-coated nanoparticles (QSNs) and phosphor silicone gel has been proved to be dramatically improved, there are few literatures referring to the reduction of QDs' working temperature.

Therefore, in this work, a separated QSNs/phosphor structure, which composed of a QSNs-on-chip layer with a yellow phosphor layer above, was proposed to reduce the QDs working temperature. Figure 1 shows the schematic of QSNs-on-chip WLEDs (type I) and conventional QSNs/phosphor mixed WLEDs (type II). Red-emissive CdSe/ZnS core–shell QDs were synthesized, and QSNs were prepared by a micro-emulsion reaction. For the fabrication of QSNs-on-chip WLEDs packaging, QSNs were

[1]Corresponding author.

Contributed by the Electronic and Photonic Packaging Division of ASME for publication in the Journal of Electronic Packaging. Manuscript received September 27, 2018; final manuscript received November 19, 2018; published online April 10, 2019. Assoc. Editor: Changqing Chen.

  

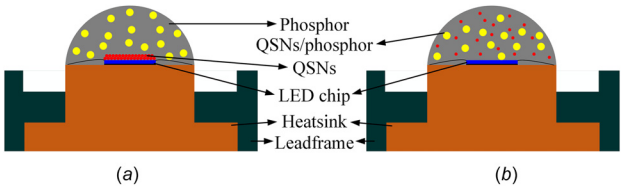


**Fig. 1 Schematic of the (*a*) QSNs-on-chip and (*b*) mixed type WLEDs. (*a*) QSNs-on-chip and (*b*) QSNs/phosphor mixed.**

directly coated onto the LED chip; then, yellow-emissive YAG:Ce phosphor silicone gel was coated. Both thermal simulations and thermal infrared temperature measurements were conducted to analyze the optical and thermal performances of this newly proposed WLEDs packaging.

## 2 Experimental Setup

**2.1 Preparation of Quantum Dots at Silica Nanoparticles.** Red-emissive CdSe/ZnS core/shell QDs were prepared by our proposed Tri-*n*-octylphosphine (TOP)-assisted successive ionic layer adsorption and reaction method [17]. This synthesis route enables the high quantum yields of QDs at high coverage of the shell.

To coat the QDs with silica shells, a micro-emulsion reaction was applied [18]. Figure 2 shows the schematic of silica coating process. Briefly, 25 ml of cyclohexane as a solvent and 3 g of IGEPAL CO-520 (Sigma-Aldrich, Beijing, China) as a surfactant were mixed at room temperature. 0.5 mg of QDs dispersed in 0.5 ml of toluene were introduced into the above mixture, and then 0.5 ml (9 mmol) of tetraethyl orthosilicate was added. The reaction was initiated by adding 0.5 ml of ammonium at the rate of 0.2 ml/min and then it was allowed to proceed for 40 h. After completion of the silica growth, the solution was precipitated by adding methanol and was centrifuged to isolate the QSNs from the microemulsion. The resultant QSNs were washed sequentially with cyclohexane, *n*-hexane and finally dispersed in methanol.

**2.2 Fabrication of White Light-Emitting Diodes.** In the fabrication of QSNs-on-chip WLEDs, QSNs methanol solution was first dropped onto the InGaN LED chip (455 nm), then the module was placed on the hotplate at 70 °C for 10 min. After all the methanol was evaporated, YAG:Ce phosphor (538 nm; Intematix, Co., Fremont, CA) was mixed homogenously with silicone gel (Dow Corning OE 6550, A:B = 1:1). Bubbles introduced during the mixing process were removed by applying alternating cycles of vacuum. Then the phosphor gel was coated onto the LED module to cover the LED chip and QSNs. Finally, the phosphor gel was cured by an annealing step at 150 °C for 30 min.

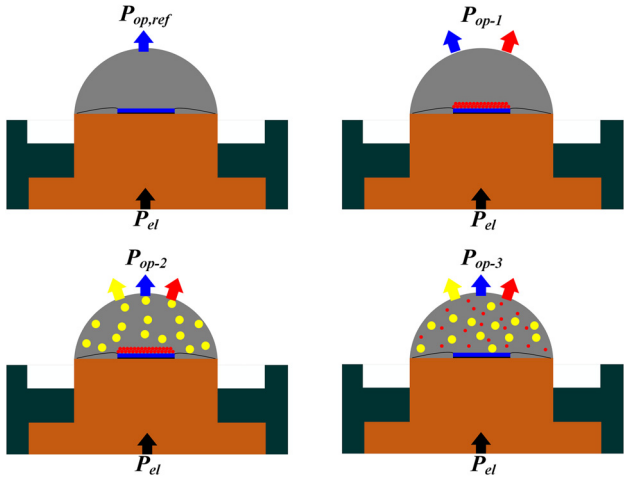


**Fig. 3 Schematic showing the heat generation measuring processes**

As a comparison, the mixed-type WLEDs were also fabricated. First, QSNs methanol solution was mixed homogenously with phosphor silicone gel. Then the methanol solvent was removed by applying 60 °C heating and vacuum alternately. After all the methanol was evaporated, the resultant was coated onto the LED chip, followed by an annealing step at 150 °C for 30 min. For convenience, the QSNs-on-chip WLEDs were labeled as type I, and those of mixed type were labeled as type II.

**2.3 Measurement of Heat Generation.** Figure 3 shows the schematic of the heat power measuring process. First, the optical power of two types of WLEDs were measured by an integrating sphere (ATA-1000; Everfine, Corp., Hangzhou, China), and then the heat power of LED chip ($Q_{chip}$), QSNs ($Q_{QSNs}$), phosphor silicone gel ($Q_{phosphor}$), and QSNs/phosphor–silicone gel ($Q_{QSNs/phosphor}$) were calculated according to the optical losses of the corresponding layer [19]

$$Q_{chip} = P_{el} - P_{op,ref} \tag{1}$$

$$Q_{QSNs} = P_{op,ref} - P_{op-1} \tag{2}$$

$$Q_{phosphor} = P_{op-1} - P_{op-2} \tag{3}$$

$$Q_{QSNs/phosphor} = P_{el} - P_{op-3} \tag{4}$$

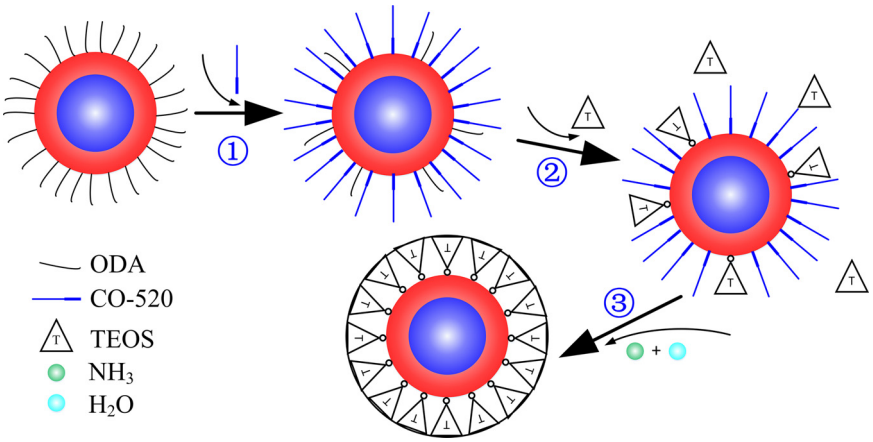


**Fig. 2 Schematic of the silica coating process**

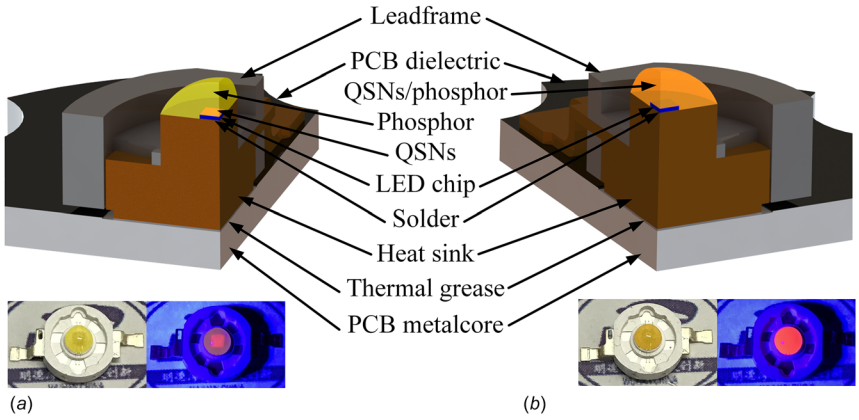


**Fig. 4 Finite element models setup of (*a*) QSNs-on-chip and (*b*) mixed type WLEDs. The insets show the corresponding photographs of the WLEDs under daylight and ultraviolet (UV) light. (*a*) Type I: QSNs-on-chip and (*b*) type II: QSNs/phosphor mixed.**

where $P_{el}$ is the input electric power, $P_{op,ref}$ is the optical power from WLEDs with only silicone, $P_{op\text{-}1}$ is the optical power from WLEDs with QSNs and silicone, $P_{op\text{-}2}$ is the optical power from the type I WLEDs, $P_{op\text{-}3}$ is the optical power from the type II WLEDs. Herein, the optical losses in lead frame are negligible due to their high reflectance and low absorption, and the scattering coefficient of QDs is assumed to be zero due to their small size [20]. Besides, it is assumed that the entire optical power loss is converted into heat power within each layer [21,22].

**2.4 Thermal Simulation Setup.** Finite element models (FEM) of two WLEDs were built to conduct the thermal simulations, as depicted in Fig. 4. The WLEDs were mounted onto a metal-core printed circuit board (PCB) for electrical connection and heat dissipation. Thickness and thermal conductivity of each component used for simulation are listed in Table 1.

The thermal conductivity of QSNs was calculated by [23]

$$K_{QSNs} = \frac{k_{silica}M^2}{(M-\gamma)\ln(1+M)+\gamma M} \tag{5}$$

With $M = \varepsilon_p(1+\gamma)-1$, where $\varepsilon_p = k_{QDs}/k_{silica}$ is the reduced thermal conductivity of nanoparticle and $\gamma = \delta/r_{QDs}$ is the ratio of the silica thickness to the original QDs radius. Due to the symmetry, only a quarter of the WLEDs model was utilized to simulate the temperature field. The boundary conditions of the FEM model were set as follows: the ambient temperature was fixed as 25 °C; natural convection occurred at the bottom surface of the metal-core printed circuit board with a heat transfer coefficient of 10 W/(m$^2$ K), and other surfaces were cooled by natural convection with a heat transfer coefficient of 8 W/(m$^2$ K). All the boundary conditions were similar as those in Ref. [24].

**Table 1 Thickness and thermal conductivity of each component**

| Component | Thickness (nm) | Thermal conductivity (W m$^{-1}$ K$^{-1}$) |
|---|---|---|
| PCB metalcore | 0.98 | 170 |
| Thermal grease | 0.05 | 5 |
| Heat sink | 6 | 170 |
| Solder | 0.05 | 5 |
| LED chip | 0.1 | 65.6 |
| QSNs | 0.0001 | 11.3 |
| Phosphor | 3 | 0.18 |
| QSNs/phosphor | 3 | 0.18 |
| PCB dielectric | 0.02 | 0.2 |
| Leadframe | 6 | 0.36 |

## 3 Results and Discussion

Figure 5 shows the high-resolution transmission electron microscopy images of the as-prepared CdSe/ZnS QDs and the QSNs, and the absorption/emission spectra of the core and core/shell QDs. From Fig. 5(*a*), the QDs' average size is measured as 6.4 nm with uniform size distribution. Benefited from the TOP-assisted successive ionic layer adsorption and reaction method, by which the surface lattice imperfections is avoided by the surface ions redissolution and lattice re-arrangement during the whole ZnS shell formation process, the absolute PL quantum yields were enhanced efficiently from 45% (core) to 69% (core–shell), as depicted in Fig. 5(*c*). Figure 5(*b*) shows transmission electron microscope images of the as-prepared QSNs,, which demonstrate well dispersity and uniform size distribution. The average particle size is measured as 32 nm with silica coating thickness of

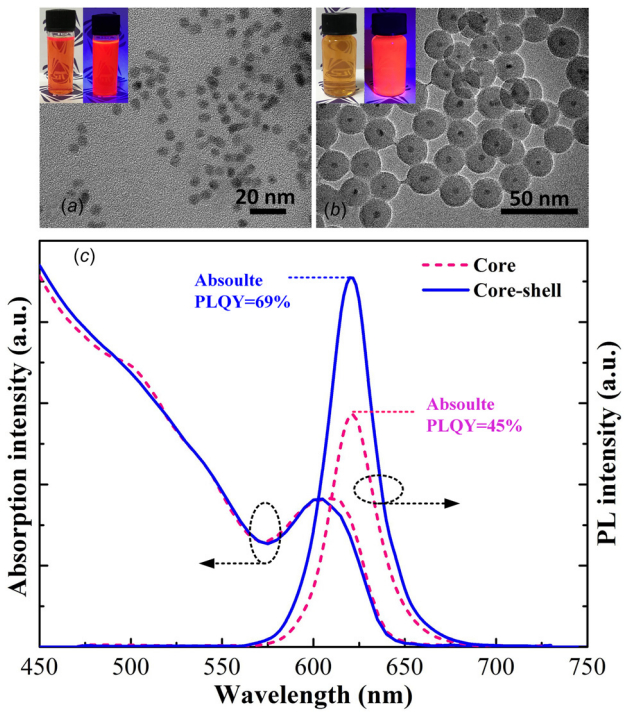


**Fig. 5 High-resolution transmission electron microscopy images of the CdSe/ZnS QDs (*a*) and the QSNs (*b*), insets show the corresponding photographs under daylight and UV light. (*c*) Absorption and PL spectra of the CdSe core QDs and CdSe/ZnS core–shell QDs.**

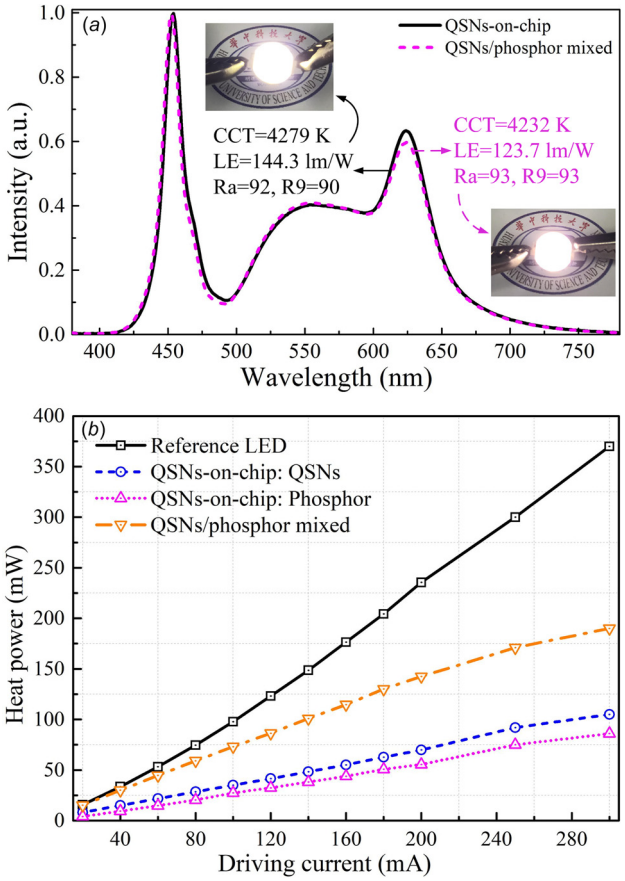


**Fig. 6 (*a*) Electroluminescence spectra of the as-fabricated WLEDs under driving current of 20 mA, insets show their illuminated photographs. (*b*) Heat generation of each component under different driving current.**

12.8 nm. This coating thickness can provide effective protection for QDs and retain the QDs' PL intensity.

Figure 6(*a*) illustrates the electroluminescence spectra of the as-fabricated WLEDs under 20 mA illumination. With similar spectral power distribution, these WLEDs present correlated color temperature around 4250 K (natural white), and high CRI of $Ra > 92$, $R9 > 90$. Note that the QSNs-on-chip WLEDs achieved high LE of 144.3 lm/W, which is 16.7% higher than that of mixed type. This is mainly attributed to the separated structure, which reduces the reabsorption losses between QSNs and phosphor particles. Figure 6(*b*) shows the current-dependent heat power in each component of QDs-WLEDs. It is seen that the heat generation in LED chip is much larger than those in QDs and phosphor. Besides, the heat generation of QSNs/phosphor in the mixed type is slightly larger than QSNs plus phosphor in the separated type. Therefore, the measured heat generation confirms the reduction of reabsorption losses by our proposed QSNs-on-chip structure.

To investigate the temperature difference between these two types of WLEDs, the measured heat generations were loaded onto the FEM and thermal simulations were conducted. Figure 7 shows the simulated temperature fields of these WLEDs under driving current. The result shows that the highest temperature of all the WLEDs locates in the top of phosphor/QSNs silicone gel. This is mainly because of the low thermal conductivity of silicone gel, and the heat generation of phosphor/QSNs cannot be quickly dissipated from WLEDs to the surrounding air. The highest temperature in type I is lower than that in type II, and this difference is more apparent at larger driving current. For instance, the temperature difference is 11.5 °C, 21.3 °C, and 30.3 °C at driving current of 80 mA, 200 mA, and 300 mA, respectively. Therefore, benefited from the proposed QSNs-on-chip configuration, the QDs working temperature can be significantly reduced.

To validate above simulation results, the corresponding temperature fields of the two WLEDs were measured by an infrared thermal imager (FLIR SC620). The emissivity of silicone gel was set

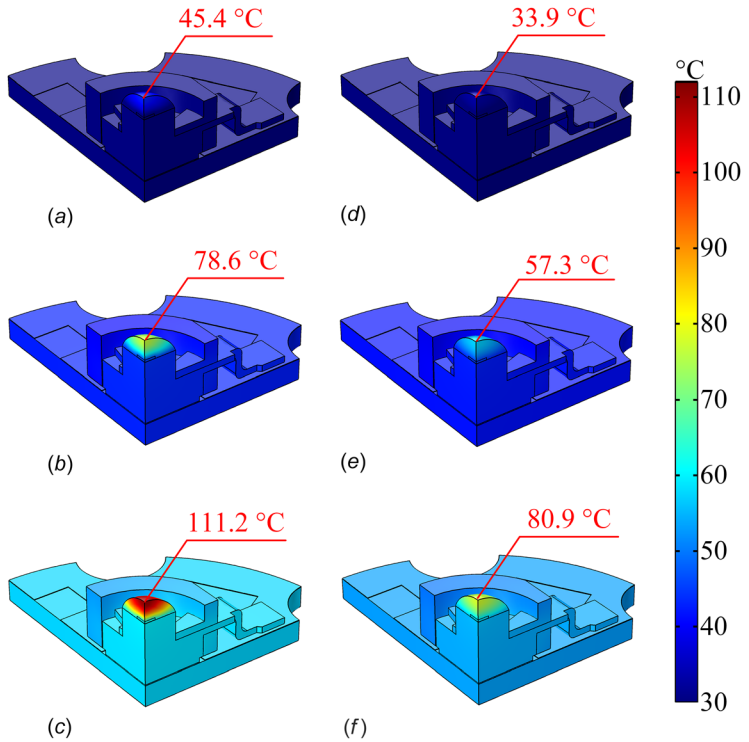


**Fig. 7 Simulated steady-state temperature fields of two WLEDs under driving current of 80 mA, 200 mA, and 300 mA. (*a*) Mixed at 80 mA, (*b*) mixed at 200 mA, (*c*) mixed at 300 mA, (*d*) QSNs on-chip at 80 mA, (*e*) QSNs on-chip at 200 mA, and (*f*) QSNs on-chip at 300 mA.**

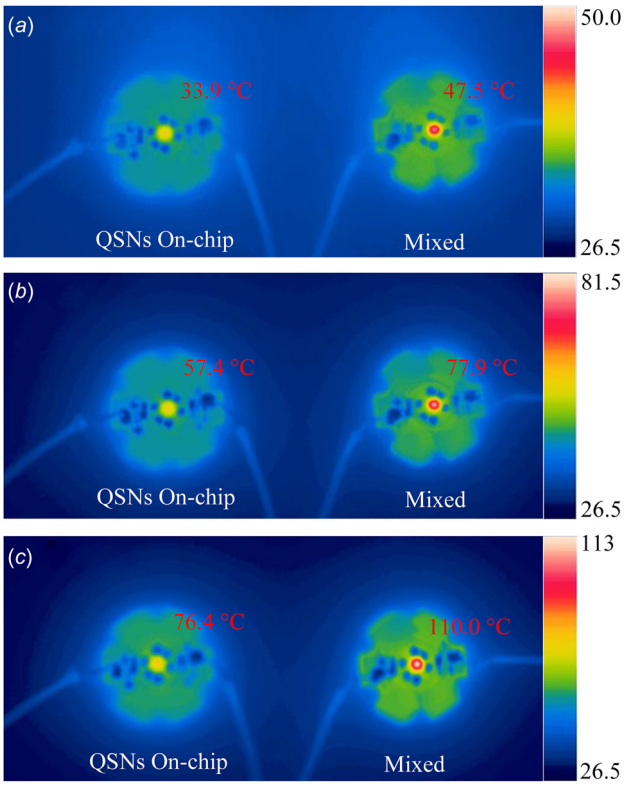


**Fig. 8 Temperature fields of two WLEDs under driving current of (*a*) 80 mA, (*b*) 200 mA, and (*c*) 300 mA**

as 0.96 [25], and the distance between WLEDs and the camera lens was fixed as 0.3 m. All the temperature fields were obtained after the WLEDs were lighted up for 30 min. Figure 8 shows the measured steady-state temperature fields. It is seen that the simulated temperature distributions between these WLEDs agree well with the experimental results, and the maximum relative deviation of the highest temperature between experimental and simulation results is 5.9% (76.4 °C and 80.9 °C at 300 mA). Therefore, it was confirmed by the experimental results that the highest temperature in QSNs-on-chip type is lower than that in the conventional mixed type.

## 4 Conclusions

In this work, a separated QSNs/phosphor structure, composed of a QSNs-on-chip layer below a yellow phosphor layer, was proposed to reduce the QDs working temperature. A silica shell was coated onto the QDs surface to solve the compatibility problem between QDs and silicone. With CRI > 92 and R9 > 90, the newly proposed QSNs-based WLEDs present 16.7% higher LE and lower QDs working temperature over conventional mixed-type WLEDs. The reduction of QDs' temperature can reach 11.5 °C, 21.3 °C, and 30.3 °C at driving current of 80 mA, 200 mA, and 300 mA, respectively. Therefore, benefited from the proposed QSNs-on-chip configuration, which reduce the reabsorption losses and enhance the thermal dissipation condition of QSNs, the QDs working temperature can be significantly reduced, so as to prolong the lifetime of QDs.

## Funding Data


- National Natural Science Foundation of China (Grant Nos. 51625601, 51576078, and 51606074; Funder ID: 10.13039/501100001809).
- The Ministry of Science and Technology of the People's Republic of China (Project No. 2017YFE0100600; Funder-ID: 10.13039/501100002855).
- The financial support from Creative Research Groups Funding of Hubei Province (Award No. 2018CFA001; Funder ID: 10.13039/501100003819).
- The Shenzhen Innovation Project (Award Nos. KC2014JSQN0011A and KQCX20140522151322950; Funder-ID: 10.13039/501100010877).
- The Graduates' Innovation Fund, Huazhong University of Science and Technology (No. 5003120016; Funder ID: 10.13039/501100003397).


## References


[1] Pimputkar, S., Speck, J. S., DenBaars, S. P., and Nakamura, S., 2009, "Prospects for LED Lighting," Nat. Photonics, **3**(4), pp. 180–182.

[2] Luo, X., Hu, R., Liu, S., and Wang, K., 2016, "Heat and Fluid Flow in High-Power LED Packaging and Applications," Prog. Energy Combust. Sci., **56**, pp. 1–32.

[3] Jang, H. S., and Jeon, D. Y., 2007, "White Light Emission From Blue and Near Ultraviolet Light-Emitting Diodes Precoated With $Sr_3SiO_5$: $Ce^{3+}$, $Li^+$ Phosphor," Opt. Lett., **32**(23), pp. 3444–3446.

[4] Jang, H. S., Im, W. B., Lee, D. C., Jeon, D. Y., and Kim, S. S., 2007, "Enhancement of Red Spectral Emission Intensity of $Y_3Al_5O_{12}$:$Ce^{3+}$ Phosphor Via Pr Co-Doping and Tb Substitution for the Application to White LEDs," J. Lumin., **126**(2), pp. 371–377.

[5] Uheda, K., Hirosaki, N., and Yamamoto, H., 2006, "Host Lattice Materials in the System $Ca_3N_2$-AlN-$Si_3N_4$ for White Light Emitting Diode," Phys. Status Solidi A, **203**(11), pp. 2712–2717.

[6] Dhanaraj, J., Jagannathan, R., and Trivedi, D. C., 2003, "$Y_2O_2S$: $Eu^{3+}$ Nanocrystals-Synthesis and Luminescent Properties," J. Mater. Chem., **13**(7), pp. 1778–1782.

[7] Cho, K.-S., Lee, E. K., Joo, W.-J., Jang, E., Kim, T.-H., Lee, S. J., Kwon, S.-J., Han, J. Y., Kim, B.-K., Choi, B. L., and Kim, J. M., 2009, "High-Performance Crosslinked Colloidal Quantum-Dot Light-Emitting Diodes," Nat. Photonics, **3**(6), pp. 341–345.

[8] Xie, B., Hu, R., and Luo, X., 2016, "Quantum Dots-Converted Light-Emitting Diodes Packaging for Lighting and Display: Status and Perspectives," ASME J. Electron. Packag., **138**(2), p. 020803.

[9] Chen, W., Wang, K., Hao, J., Wu, D., Qin, J., Dong, D., Deng, J., Li, Y., Chen, Y., and Cao, W., 2016, "High Efficiency and Color Rendering Quantum Dots White Light Emitting Diodes Optimized by Luminescent Microspheres Incorporating," Nanophotonics, **5**(4), pp. 565–572.

[10] Xie, B., Zhang, J., Chen, W., Hao, J., Cheng, Y., Hu, R., Wu, D., Wang, K., and Luo, X., 2017, "Realization of Wide Circadian Variability by Quantum Dots-Luminescent Mesoporous Silica-Based White Light-Emitting Diodes," Nanotechnology, **28**(42), p. 425204.

[11] Kim, H., Jang, H. S., Kwon, B. H., Suh, M., Kim, Y., Cheong, S. H., and Jeon, D. Y., 2011, "In Situ Synthesis of Thiol-Capped $CuInS_2$-ZnS Quantum Dots Embedded In Silica Powder by Sequential Ligand-Exchange and Silanization," Electronchem. Solid-State Lett., **15**(2), pp. K16–K18.

[12] Tamborra, M., Striccoli, M., Comparelli, R., Curri, M. L., Petrella, A., and Agostiano, A., 2004, "Optical Properties of Hybrid Composites Based on Highly Luminescent CdS Nanocrystals in Polymer," Nanotechnology, **15**(4), pp. S240–S244.

[13] Zhang, H., Cui, Z., Wang, Y., Zhang, K., Ji, X., Lu, C., Yang, B., and Gao, M., 2003, "From Water-Soluble CdTe Nanocrystals to Fluorescent Nanocrystal-Polymer Transparent Composites Using Polymerizable Surfactants," Adv. Mater., **15**(10), pp. 777–780.

[14] Chen, W., Wang, K., Hao, J., Wu, D., Wang, S., Qin, J., Li, C., and Cao, W., 2015, "Highly Efficient and Stable Luminescence From Microbeans Integrated With Cd-Free Quantum Dots for White-Light-Emitting Diodes," Part. Part. Syst. Charact., **32**(10), pp. 922–927.

[15] Zhao, B., Yao, X., Gao, M., Sun, K., Zhang, J., and Li, W., 2015, "Doped Quantum Dots@Silica Nanocomposites for White Light-Emitting Diodes," Nanoscale, **7**(41), pp. 17231–17236.

[16] Zhou, C., Shen, H., Wang, H., Xu, W., Mao, M., Wang, S., and Li, L. S., 2012, "Synthesis of Silica Protected Photoluminescence QDs and Their Application for Transparent Fluorescent Films With Enhanced Photochemical Stability," Nanotechnology, **23**(42), p. 425601.

[17] Hao, J., Zhou, J., and Zhang, C., 2013, "A Tri-*n*-Octylphosphine-Assisted Successive Ionic Layer Adsorption and Reaction Method to Synthesize Multilayered Core-Shell CdSe-ZnS Quantum Dots With Extremely High Quantum Yield," Chem. Comm., **49**(56), pp. 6346–6348.

[18] Li, H., Wu, K., Lim, J., Song, H. J., and Klimov, V. I., 2016, "Doctor-Blade Deposition of Quantum Dots Onto Standard Window Glass for Low-Loss Large-Area Luminescent Solar Concentrators," Nat. Energy, **1**, p. 16157.

[19] Xie, B., Chen, W., Hao, J., Wu, D., Yu, X., Chen, Y., Hu, R., Wang, K., and Luo, X., 2016, "Structural Optimization for Remote White Light-Emitting Diodes With Quantum Dots and Phosphor: Packaging Sequence Matters," Opt. Express, **24**(26), pp. A1560–A1570.

[20] Şahin, D., Ilan, B., and Kelley, D. F., 2011, "Monte Carlo Simulations of Light Propagation in Luminescent Solar Concentrators Based on Semiconductor Nanoparticles," J. Appl. Phys., **110**(3), p. 033108.
[21] Xie, B., Liu, H., Hu, R., Wang, C., Hao, J., Wang, K., and Luo, X., 2018, "Targeting Cooling for Quantum Dots in White QDs-LEDs by Hexagonal Boron Nitride Platelets With Electrostatic Bonding," Adv. Funct. Mater., **28**(30), p. 1801407.
[22] Ma, Y., Lan, W., Xie, B., Hu, R., and Luo, X., 2018, "An Optical-Thermal Model for Laser-Excited Remote Phosphor with Thermal Quenching," Int. J. Heat Mass Transfer, **116**, pp. 694–702.
[23] Xie, H., Fujii, M., and Zhang, X., 2005, "Effect of Interfacial Nanolayer on the Effective Thermal Conductivity of Nanoparticle-Fluid Mixture," Int. J. Heat Mass Transfer, **48**(14), pp. 2926–2932.
[24] Hu, R., Luo, X., and Zheng, H., 2012, "Hotspot Location Shift in the High-Power Phosphor-Converted White Light-Emitting Diode Packages," Jpn. J. Appl. Phys., **51**(9S2), p. 09MK05.
[25] Orloff, L., De Ris, J., and Markstein, G. H., 1975, "Upward Turbulent Fire Spread and Burning of Fuel Surface," Proc. Combust. Inst., **15**(1), pp. 183–192.